

## A SURVEY OF TOTAL SUSPENDED MATTER IN THE SOUTHERN NORTH SEA BASED ON THE 2001 SEAWIFS DATA

*Marieke A. Eleveld, Reinold Pasterkamp and Hans J. van der Woerd*

Vrije Universiteit Amsterdam, Institute for Environmental Studies (VU-IVM),  
De Boelelaan 1087, 1081 HV Amsterdam, The Netherlands;  
[marieke.eleveld/reinold.pasterkamp/hans.van.der.woerd@ivm.vu.nl](mailto:marieke.eleveld/reinold.pasterkamp/hans.van.der.woerd@ivm.vu.nl)

### ABSTRACT

Assessing the spatio-temporal distribution of total suspended matter (TSM) concentrations is important for management of the North Sea. Especially, information on supply, transport, and deposition of TSM is required. TSM in the North Sea was studied with Sea-viewing Wide Field-of-view Sensor (SeaWiFS) Level 1A Local Area Coverage (LAC) data. All SeaWiFS data covering the southern North Sea for 2001 were acquired and processed using the SeaWiFS Data Analysis System (SeaDAS 4.0) with MUMM's turbid water extended atmospheric correction algorithm. Subsequently, the POWERS TSM algorithm was used to derive TSM concentration (in  $\text{mg l}^{-1}$ ) from SeaWiFS sub-surface irradiance reflectance,  $R(0^-)$ , in band 5. Seasonal variation in TSM concentration was extracted from composites, and statistics on TSM concentrations were produced for any location within the research area. Persistent high TSM concentrations were found near the Flemish Banks and the German Bight, and in the Greater Thames Estuary and East-Anglian Plume. Supply of TSM came from fluvial input, erosion of coastal areas and resuspension from bottom sediments, and primary production. Combining TSM concentration with knowledge of the general circulation in the North Sea yielded information on surficial (net) TSM transport. On the other hand, currents and the position of fronts were also derived from patterns in TSM concentrations. Settling and subsequent deposition of TSM occurred at times with low current velocity and little wave action. An example of TSM settling after storm was also perceived. The results show that SeaWiFS images are an excellent source for the monitoring of TSM concentrations in the North Sea, and that information on supply, transport, and settling of TSM can be derived.

**Keywords:** Suspended Particulate Matter (SPM), seston, large-scale processes, Dutch coast, East-Anglian Plume.

### INTRODUCTION

Total Suspended Matter (TSM) can be defined as all matter that stays on a 0.4 to 0.5  $\mu\text{m}$  pore size filter (1). Changes in TSM concentrations and TSM transport can have important consequences for coastal zone management. Silt and clay (mud) can siltate on tidal flats and clog navigation channels and harbours, whereas sand can be an important resource for coastal defence. The quality and quantity of TSM can have direct and indirect effects on environmentally sensitive areas by pollutants attached to sediments, and by influencing the light conditions in the water, causing a decline of filter feeding organisms, submerged aquatic vegetation and plankton, subsequently affecting fish and bird populations (2). A typical TSM concentration for the North Sea of  $5 \text{ g m}^{-3}$  corresponds with a euphotic layer, where photosynthesis occurs, of 18 m depth. Despite the importance of TSM, and notwithstanding that it has been monitored through point sampling with buoys and ships, there still remain major unknowns about TSM in the southern North Sea (Figure 1), because these platforms cannot cover the entire southern North Sea.

Ocean colour satellite sensors collect data that do cover the entire southern North Sea and that allow derivation of TSM concentrations from the optical properties of the sea. When light from the sun illuminates the North Sea, it is subject to various optical interactions such as absorption and scattering; the intensity of these interactions depends on the concentrations of substances in the water. A net result from these optical interactions is that light radiates from the North Sea as water-leaving radiance,  $L_w$ . SeaWiFS is a spectro-radiometer that measures radiance in specific bands of

the light spectrum so that, after atmospheric correction, TSM concentrations can be derived. However, TSM as derived from satellites does not only comprise suspended sediment; it can also contain dissolved organic matter (CDOM), and chlorophyll (CHL) from algae. In addition, remote sensing only shows TSM concentrations over a certain near-surface layer of the North Sea. The depth of this near-surface layer varies with the depth of the water column that still scatters light to the sensor; thus the vertical diffuse attenuation coefficient of downward irradiance ( $K_d$ ) has implications for remote sensing. About 90 % of the diffusely reflected light from a water body comes from a near-surface layer of water depth  $1/K_d$ , which equals 4 m for a TSM concentration of  $5 \text{ g m}^{-3}$  in the North Sea.

One of the most successful ways to exploit remote sensing data sets is to construct compilations and atlantes (3). Material prepared for an atlas of TSM concentrations covering the southern North Sea over one year, 2001, for Dutch coastal managers formed the basis for the current study (4). This paper aims at elaborating on the information on TSM in the southern North Sea that was derived from this data set. Specific research objectives were to investigate whether the satellite data can shed more light on the supply, transport and settling of TSM in the southern North Sea, and whether ocean colour observations can supply additional information about its circulation in the southern North Sea. Knowledge of these parameters is not only of scientific interest, but also, as previously mentioned, relevant to the management of the North Sea.

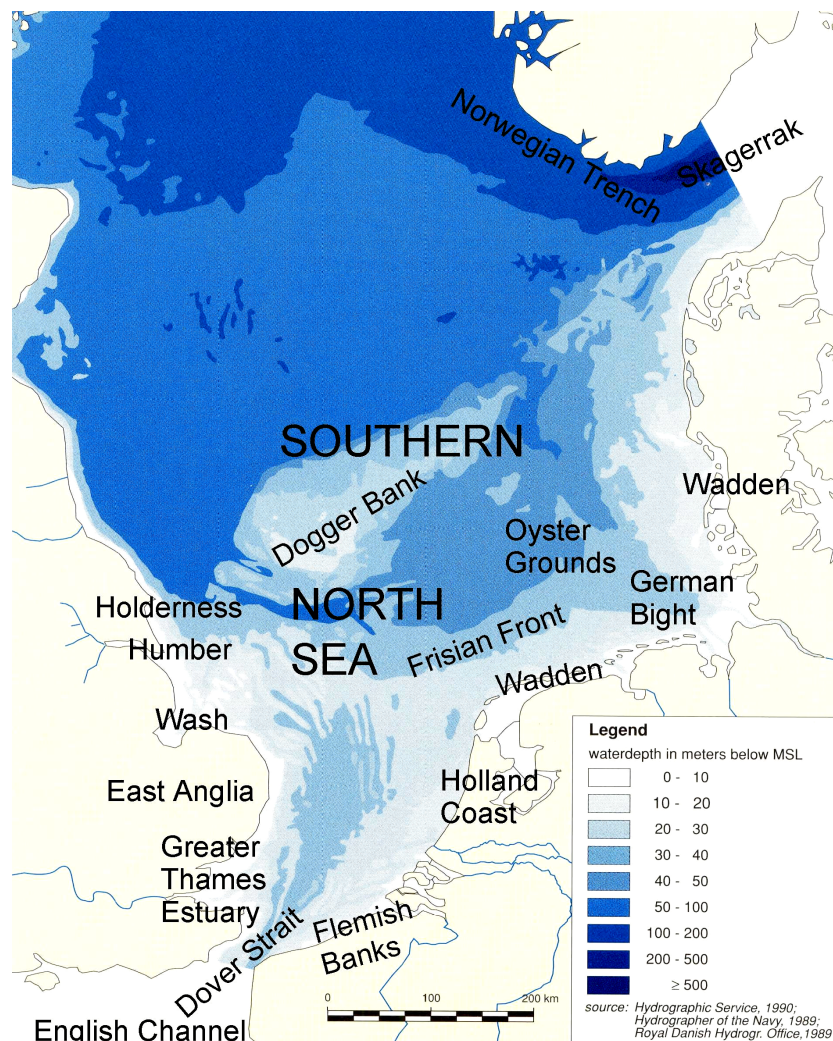


Figure 1: Research area shown on a bathymetric backdrop map (5).

**METHODS**

Sensors consisting of spectro-radiometers suitable for determining ocean colour measure radiance at sensor,  $L_{rs}$ , resulting in Level 1A data. The collected data are sent to ground stations. In this study Sea-viewing Wide Field-of-view (SeaWiFS) data from the Dundee ground station were used. Subsequent processing of these data in IVM's processing chain (Figure 2) is elaborated in this section.

First the Level 1A High Resolution Picture Transmission (HRPT) data were obtained free of charge from NASA by File Transfer Protocol (FTP). The files contained radiance counts for the eight SeaWiFS bands, additional calibration and navigation data, instrument and spacecraft telemetry, and ancillary data on wind, surface pressure, humidity, and ozone. Then the data sets having the southern North Sea in a central position on the images were selected based on filtering on file-names, which carry information about the time of overpass.

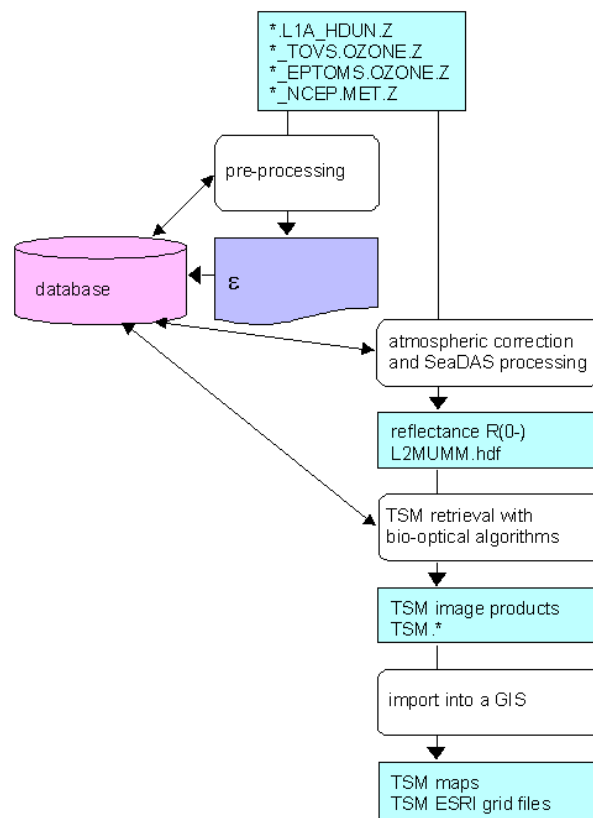


Figure 2: IVM's processing chain.

Subsequently this data set was pre-processed. Radiance at sensor,  $L_{rs}$ , is a measurement of light from the water and from the atmosphere. The atmosphere over coastal regions differs from the ocean atmosphere, and the amount of TSM in coastal waters differs from the amount in the ocean. Therefore, an extension to the standard SeaWiFS Data Analysis System (SeaDAS) atmospheric correction method had to be used to get values for the calibration parameters aerosol reflectance ratio MUMM-epsilon ( $\epsilon$ ), and water reflectance ration MUMM-alpha. The MUMM atmospheric correction algorithm for turbid waters (6) uses aerosol radiance in two SeaWiFS bands within the near-infrared reach, band 7 (745-785 nm) and band 8 (845-885 nm). Scatter plots of band 7:8 Rayleigh-corrected reflectances representing the ratio of aerosol path reflectance gave values for the calibration parameters on an image-by-image basis. Points with low reflectance on the scatter plot are dominated by aerosol path reflectance. These points were used to determine MUMM-epsilon for each image in the data set. MUMM-alpha, water-leaving reflectance of very turbid water, was taken default as 1.72.

Using these parameters, subsequent processing in SeaDAS generates atmospherically corrected Level 2 data, subsurface irradiance reflectance  $R(0^-)$  of the southern North Sea. From this intermediate product, water quality parameters can be derived.

In this case the IVM-POWERS TSM algorithm was used. This algorithm (7,8) was based on the Gordon model (9) and calibrated with Specific Inherent Optical Properties (SIOPs) of the North Sea (10). The Gordon model is a bio-optical model that describes the relationship between the amount of upwelling light just below the water surface, here expressed as subsurface irradiance reflectance ( $R(0^-)$ ), and the optical properties of water and its constituents TSM, CHL, and CDOM through SIOPs, which are related to absorption ( $a$ ) and backscatter ( $b_b$ ).

$$R(0^-) = f \cdot \frac{b_b}{a + b_b}$$

(The coefficient  $f$  can vary due to solar angle, scattering at a certain angle relative to total scattering (scattering phase function), and viewing geometry (9))

#### Elaboration of the bio-optical modelling

The Gordon (1975) reflectance model (9) predicts subsurface irradiance reflectance as a function of the inherent optical properties (IOPs) absorption ( $a$ ) and backscatter ( $b_b$ ). Absorption and backscatter of natural water are expressed in terms of the constituents of the water as follows:

$$a = a_w + a_{CHL}^* CHL + a_{TSM}^* TSM + a_{CDOM}^* CDOM$$

$$b_b = b_{b,w} + b_{b,TSM}^* TSM$$

Absorption and backscattering are linear functions of the concentrations of the constituents, which allows defining Specific Inherent Optical Properties (SIOP).

$$SIOP = IOP / C_{is}$$

$C_{is}$  is the *in situ* measured concentration of the respective constituent. This normalization of *in situ* measured IOPs allows to estimate the IOP at any concentration from an optical model ( $C_{om}$ ) through:

$$IOP = SIOP \cdot C_{om}$$

This can be elaborated to:

$$R(0^-) = f \cdot \frac{b_{b,w} + b_{b,TSM}^* TSM}{a_w + b_{b,w} + a_{CHL}^* CHL + (a_{TSM}^* + b_{b,TSM}^*) TSM + a_{CDOM}^* CDOM}$$

This set of equations provides the explicit relationship between the SIOP, the concentrations of the water constituents, and  $R(0^-)$ , on which the IVM-POWERS TSM algorithm was based (7).

Initially, the algorithm was parameterised with various sets of *in situ* measurements of Specific Inherent Optical Properties (SIOPs), and calibrated with TSM concentrations from the PMNS data set (11). The final, IVM-POWERS TSM algorithm was parameterised with the Belgica SIOP set (10). Band 5 (555 nm) had been chosen because of its maximal sensitivity for TSM, and minimal sensitivity to other water constituents such as concentrations of chlorophyll (CHL) and Coloured Dissolved Organic Matter (CDOM), and inaccuracies in atmospheric correction. Sensitivity analysis was performed on all factors that were assumed constant,  $f$ , and the IOPs, CHL and CDOM (7,8).

Recently the IVM POWERS TSM algorithm has been validated with a time series of *in situ* measurements TSM for three sampling stations just off the Dutch coast, at Noordwk 10, 20 and 70 (8). Kolmogorov-Smirnov tests on the distributions of TSM values showed the values from *in situ* and remote sensing data sets to be consistent with a single distribution function for Noordwk 70, while the distribution functions of the *in situ* and remote sensing samples differ for Noordwk 10 and 20.

In addition to the resulting data on TSM concentrations, TSM quick-looks were generated, and the percentage of cloud cover over the southern North Sea was provided for each image. The TSM data were re-projected to a rectangular co-ordinate system. The entire data set covering the research area in 2001 was processed with this method. This resulted in 491 TSM products: more than one image a day on average.

Based on this georeferenced TSM data set, a further analysis has been performed. Individual images are hardly ever 100 % cloud-free for the entire southern North Sea, which is one of the reasons that composites of images were made. In addition, these bimonthly composites mediate the effect of imagery being acquired during different tidal stages. Statistical analysis in Matlab provided mean, standard deviation, median, and number of samples per grid cell. The average number of sampled images per pixel is 107. Some of the data have also been exported as tables with comma separated values to enable combination with other GIS data sets.

In ArcView 3.3 with the Spatial Analyst extension, these values were imported as Event themes into a View with Universal Transverse Mercator (UTM) WGS 84 projection. The points were interpolated to grids using the Nearest Neighbour algorithm so that the closest point determined the value of the cell.

In the resulting maps, the estimated overall accuracy of the values for TSM concentrations off the Dutch and Belgian coast is about 3 – 5  $\text{g m}^{-3}$  on an average.

## RESULTS

The North Sea is characterised by persistent high TSM concentrations near the Flemish Banks and the German Bight, near the Humber Estuary, and in the Greater Thames Estuary at the head of the East Anglian Plume (Figure 3a). These high concentrations occur in different water types mainly comprising of Continental coastal water, and Scottish and English coastal water, respectively. The sea bottom occurs at depths varying from 0 to 30 m below Mean Sea Level (MSL). Persistent low sediment concentrations (Figure 3b) occur North of Dogger Bank where Northern North Sea water and Atlantic Ocean water are present, and the sea bottom is found at depths between 50 and 100m below MSL. Despite the low concentrations, there could still be a considerable amount of suspended matter present in the water integrated over the depth of the total water column. Along the Dutch coast, TSM is concentrated by residual currents in a 6 km wide band just off the coast (12), whereas relatively clear fresh water is found at the surface at about 30 to 50 km off the coast.

The collection of TSM data was studied in order to shed light on the supply, transport, and deposition of TSM in the southern North Sea, and to obtain additional information about its circulation in the southern North Sea.

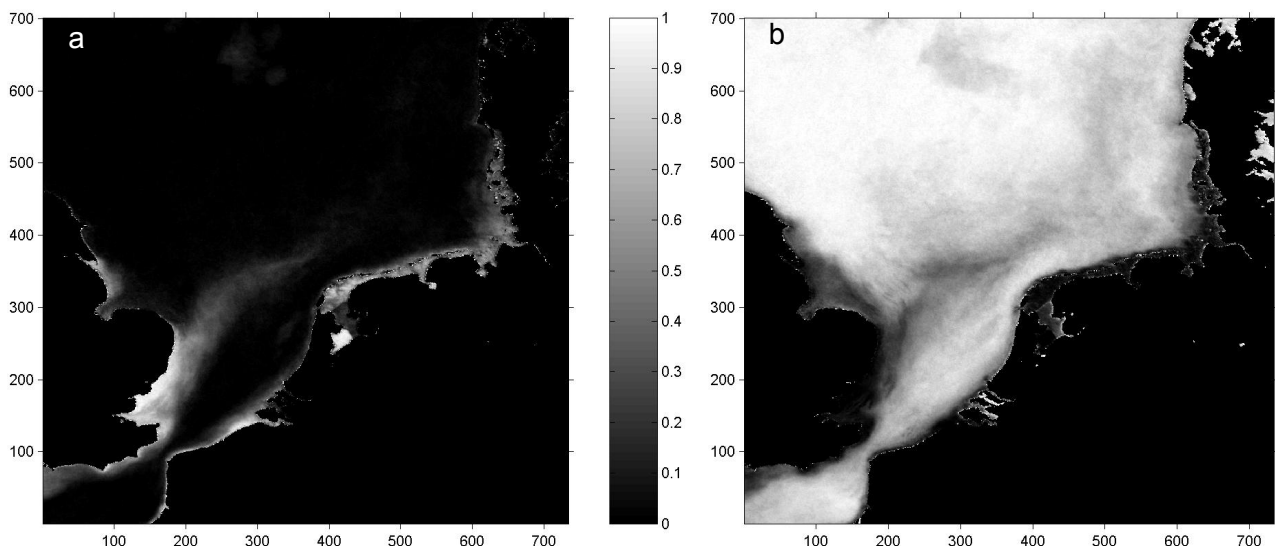


*Figure 3: Characterisation of TSM concentrations in the southern North Sea (based on 491 TSM maps for 2001). a: Persistent high TSM concentrations. Relative number of TSM maps with TSM concentrations over  $15 \text{ g m}^{-3}$ . White areas are always  $\geq 15 \text{ g m}^{-3}$ , black areas are never  $\geq 15 \text{ g m}^{-3}$ . b: Persistent low sediment concentrations. Relative number of TSM maps with TSM  $\leq 5 \text{ g m}^{-3}$ . White areas are always  $\leq 5 \text{ g m}^{-3}$ , black areas are never  $\leq 5 \text{ g m}^{-3}$ .*

**Supply**

Supply of TSM came from fluvial input (Figure 4), erosion of coastal areas and resuspension of bottom sediments (Figure 5), and primary production (Figure 6).

A local TSM plume can be perceived on the image of 2 April (Figure 4a). This plume is related to high discharge at Hook of Holland and the Haringvliet sluices (Figure 4c). A plume like this is prominent on the remote sensing images, because these images show concentrations in the surface layer. Fresh river water has a lower density than salt water so that the plume spreads mainly over the surface, and because the images were acquired during and shortly after high discharge at two coastal stations (Figure 4c), the finer sediment has not settled yet. By 3 April the TSM concentration at the surface had diminished considerably (Figure 4b). The difference between the two images may have been emphasised by the tidal conditions; at 2 April the tide was outgoing, whereas it was high tide at 3 April. The plume was not visible anymore on subsequent images.

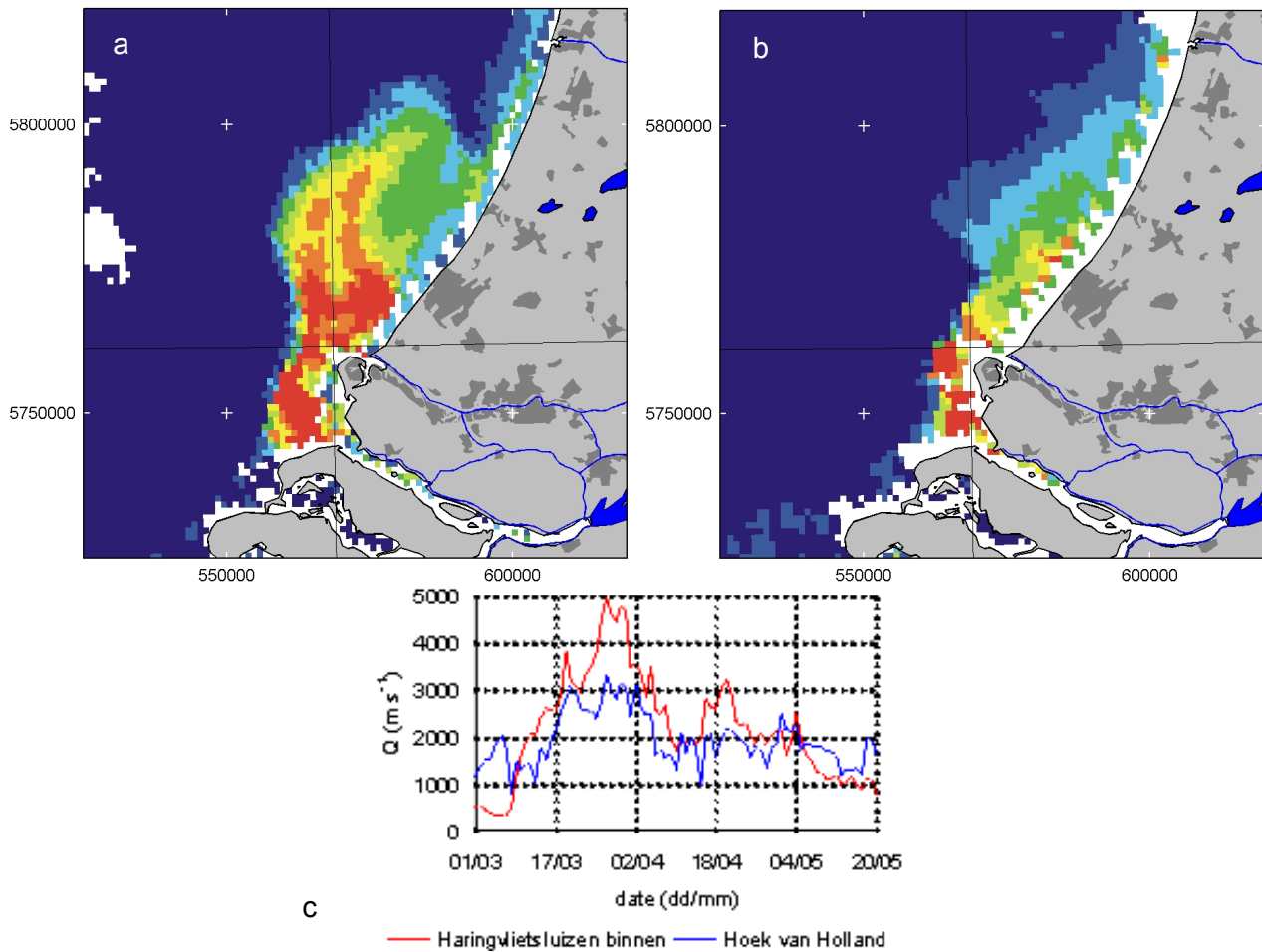


Figure 4: Supply of TSM from fluvial input. a: A local TSM plume on 2 April 2001. b: The plume is disappearing on 3 April 2001. (See Figure 5 for legend.) c: High discharge at Hook of Holland and the Haringvlietsluizen, at the mouth of the channel and the estuary, respectively (13).

A map showing means (averages) that were calculated from unclouded pixels of 81 individual images (Figure 5) illustrates sediment supply through resuspension of bottom sediments, and erosion of coastal zones. Our results show that after relatively low values of sediment concentration in summer, sediment concentrations in the surface layer increased in the September-October period. In this period, the weather becomes more unsettled (wind speed and direction are given in Figure 5), so that water layers get well mixed (also in depth), and clay and silt get re-suspended. This remobilises material that was deposited on the seafloor in summer. The wind, which forces water masses in certain directions and causes waves to stir up bottom sediments, came mostly from a southwesterly and northwesterly direction. Especially in October, hard and stormy winds from the southwest and northwest occurred. Currents coming from these directions are strengthened.

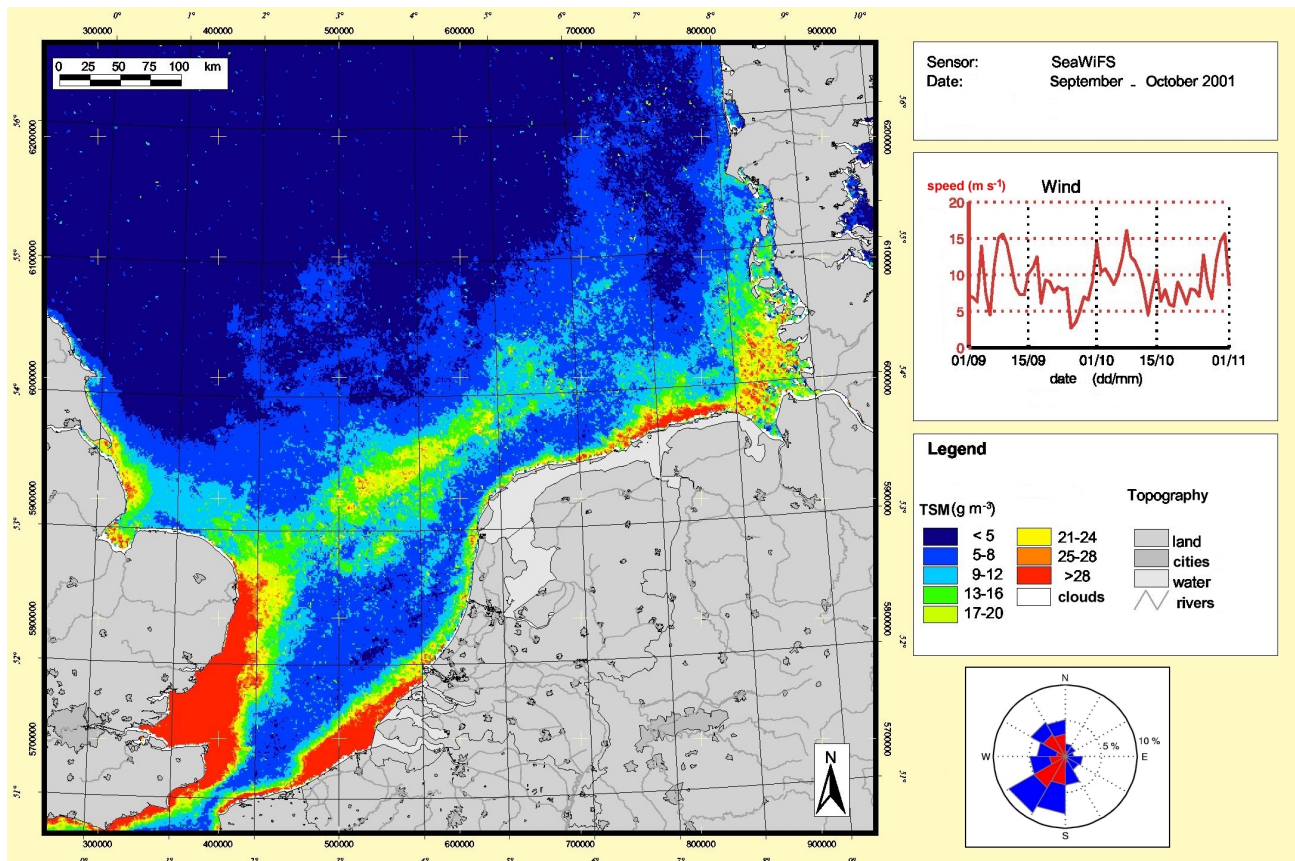


Figure 5: High TSM concentrations by resuspension. Bimonthly mean of TSM concentrations in September and October 2001. (Means were calculated from unclouded pixels of 81 individual images.) The legend, daily wind speed, and hourly relative frequency of wind direction in a wind rose are given on the right hand side. In the wind rose, blue indicates the total relative frequency, whereas red shows the relative frequency of wind speed over 10 m s<sup>-1</sup> at 'K13', a measurement station that is situated about 100 km west of Texel (14).

The naissance and growth of algae in a process also called primary production, is yet another source of TSM. Although TSM in the North Sea mainly consists of mineral particles (clay, silt and possibly some sand), locally reflectances from algae dominate when an explosive growth of algae occurs under favourable circumstances, notably when there are enough light and nutrients available and the temperature of the water suffices (15). From 5 until 28 August, an individual patch with high reflectances occurred just off the Holland coast. The sequence of images in Figure 6 shows a) the genesis of the patch on 5 August, b) the development on 11 August and, c) the decline on 28 August. A closer differentiation of TSM into mineral and organic particles with a four-band algorithm (16) confirmed that this was an algal bloom (Figure 6d).

Figure 8a is an image of 11 April. The pattern at the tail of the East-Anglian Plume is striking. This map can be compared with maps of residual currents in winter (Figure 8b) and summer (Figure 8c), in which the current has been corrected for tidal movements. They show several known currents and their boundaries, and fronts. The end of the plume seems to be confined between Scotish and English coastal water, Channel water, Central North Sea water, and Continental coastal water, but demonstrates the absence of a well-developed Frisian Front on 11 April. The latter is illustrated by the fact that the spiral at the end of the plume freely develops in north-easterly direction, instead of being redirected in an easterly direction.

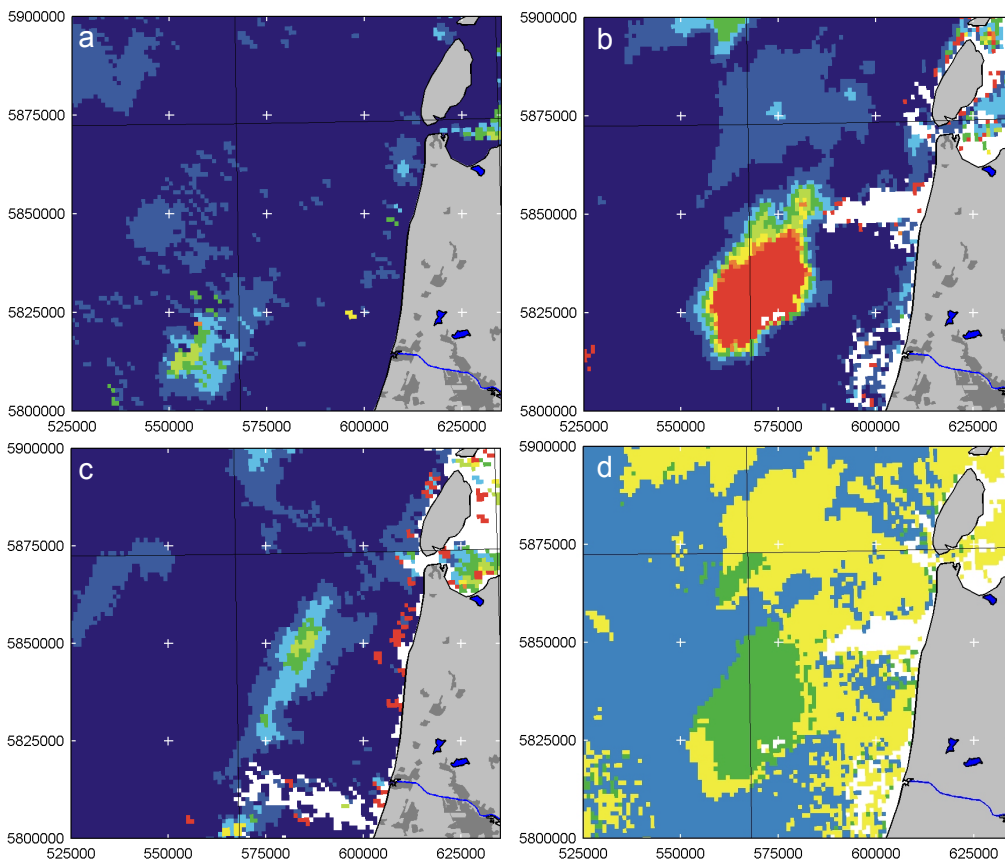


Figure 6: Supply of TSM through primary production in an algal bloom in 2001. The sequence of images show a: the genesis at 5 August, b: the development at 11 August and c: the decline at 28 August of an algal bloom just off the Holland coast. (See Figure 5 for legend.) d: green indicates algae, yellow indicates mineral material.

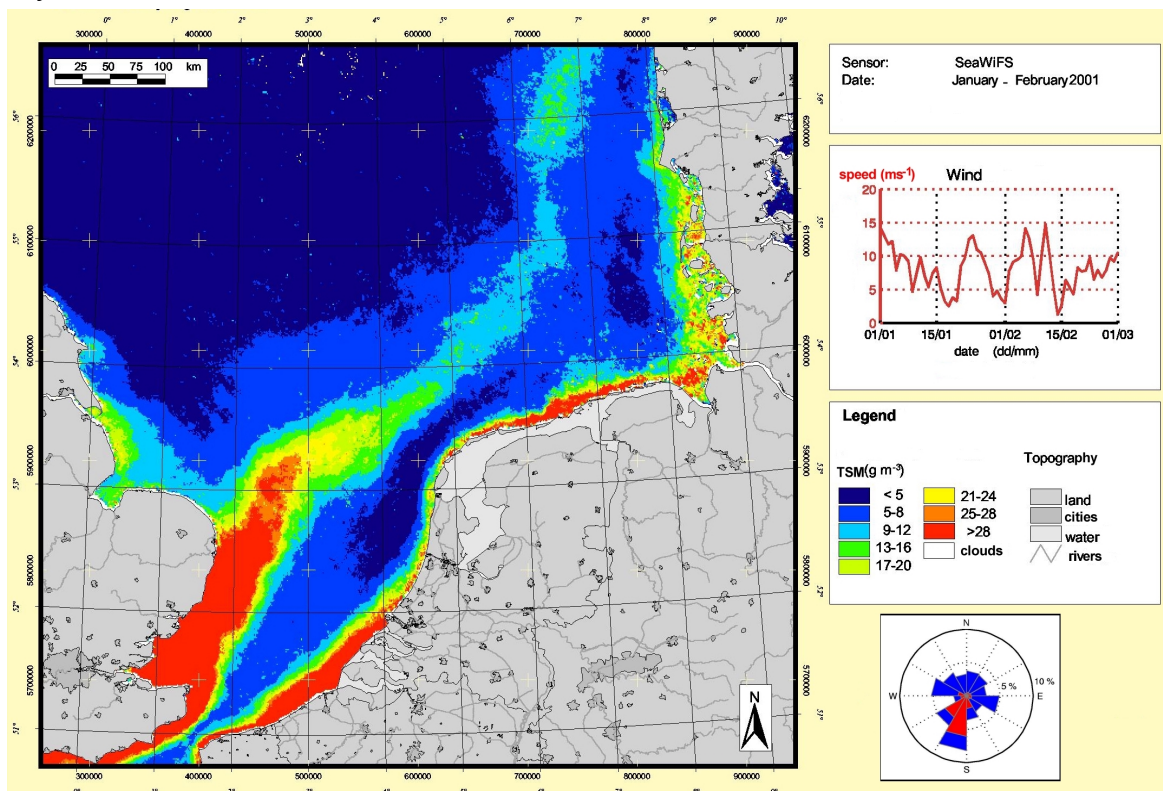


Figure 7: Mean TSM concentrations as an indicator for transport. Bimonthly mean of TSM concentrations in January and February 2001 (based on unclouded pixels of 76 individual images).

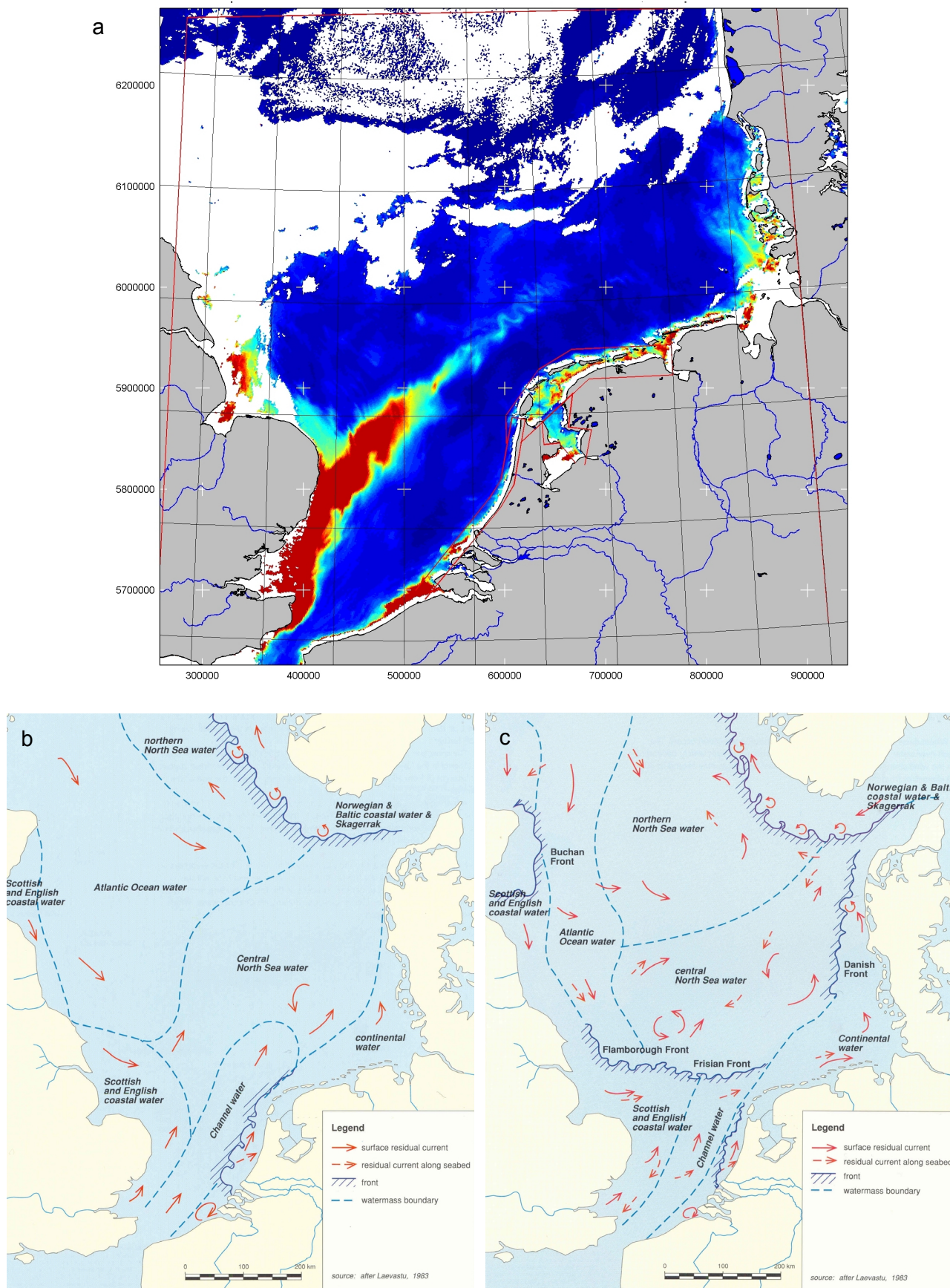


Figure 8: Derivation of currents and the position of fronts from patterns in TSM concentrations. a: TSM concentrations on 11 April 2001. (See Figure 7 for legend.) b: Residual currents, water masses and fronts in winter (5). c: Residual currents, water masses and fronts in summer (5).

**Deposition**

Settling and subsequent deposition of TSM occurred during periods of low current velocity and little wave action (Figure 9). An example of settling after storm was also perceived (Figure 10a,b).

Bimonthly mean TSM concentrations in the period March-April are lower than in January-February. The average difference per pixel is  $1.8 \text{ g m}^{-3}$ . The difference (Figure 9) results from the settling or net deposition of TSM. Additional explanations for the decrease of TSM particles in the near-surface layer could be abating supply and possibly some transport (out of the research area). The mean wind speed was lower in March-April than in January-February causing less resuspension in the former period. The relative importance of these factors should be further investigated, e.g., through validation with a numerical model of currents and suspended matter transport.

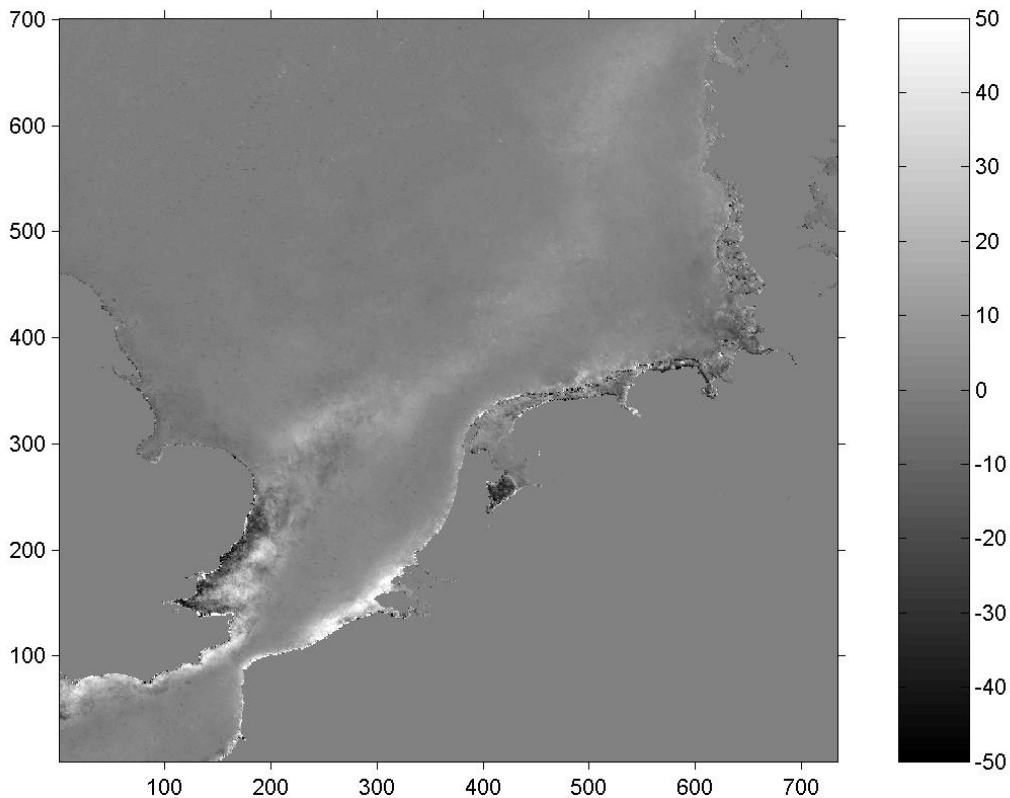


Figure 9: Difference in TSM concentrations (in  $\text{g m}^{-3}$ ) indicating net deposition. Bimonthly mean of January-February 2001 (a period with turbid water) minus the bimonthly mean of March-April 2001 (a period of low turbidity).

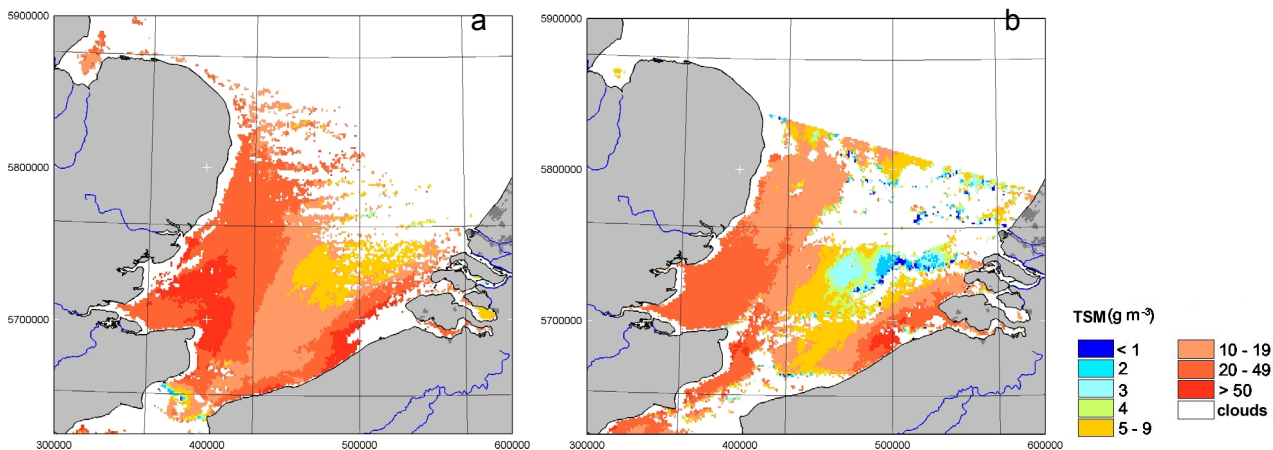


Figure 10: Settling after storm. a: High sediment concentrations during storm (28 December 2001). b: The system is restoring three days after the storm.

A (north)westerly storm, wind force 9 with strong gusts of wind occurred along the Dutch coast on 28 December. The storm was caused by a depression that moved in southeasterly direction over the North Sea and subsequently turned to the southern Baltic Sea (17). It is impossible to have a survey vessel at sea under those conditions. The satellite image (Figure 10a), however, does give information about TSM during storm. High concentrations of TSM occur over the entire surface of Dover Strait. High concentrations of larger sand particles can get into suspension during storms, but this material will settle soon when wind abates (1). On the image taken three days after the storm (Figure 10b) with northeasterly wind force 4, high TSM concentrations occur again in two separate zones, one along the English coast and Frisian Front and another along the French, Belgian and Dutch coast, separated by a zone of low concentrations at Dover Strait. The average difference in TSM concentration during and after storm is  $10.7 \text{ g m}^{-3}$  per pixel.

## CONCLUSIONS

### Concentrations

The results show that SeaWiFS images are an excellent source for monitoring TSM concentrations in the North Sea. Persistent high TSM concentrations at the surface (Figure 3a) are found in places where a lot of sediment is also available from both older geological deposits and recent supply, e.g., near estuaries, and at the Flemish Banks and the German Bight. These high concentrations occur in different coastal water types with sea bottom depths varying from 0 to 30 m below Mean Sea Level (MSL) so that resuspension of bottom sediments is still possible. Persistent low sediment concentrations at the surface (Figure 3b) occur in northern North Sea water and Atlantic Ocean water, where the sea bottom is at depths between 50 and 100 m below MSL. Despite the low concentrations, a considerable amount of suspended matter could still be present when the concentration is integrated over the full length of the water column.

For our study, the estimated overall accuracy of the values for TSM concentrations off the Dutch and Belgian coast is about  $3 - 5 \text{ g m}^{-3}$  on an average. Because of spatial dependencies, the accuracy of the relative differences between the pixels is higher, so that patterns can be mapped accurately. The mapped difference in bimonthly mean TSM concentrations (Figure 9) seems also relevant, since a very similar pattern was found for the year 2000 (with an average difference per pixel of  $3.8 \text{ g m}^{-3}$ ). The TSM algorithm was calibrated with field measurements off the Dutch and Belgian coast (10). These field measurements did not cover the full spatial variability in SIOPs of the North Sea. Therefore, the accuracy of values at other locations, such as those occurring off the English coast will be less, amongst others because TSM has a different mineral composition (19) and, therefore, different optical properties. Validation with *in situ* measurements (see also the Methods section and Van der Woerd & Pasterkamp (8)) remains a challenge, because *in situ* data sets also have their inaccuracies. For example, König et al. (18) give means with standard deviations of  $0.54 \pm 0.17 \text{ mg l}^{-1}$  (total over 8.5, 17.0 and 24.7 m depth), and  $2.0 \pm 1.3$ ,  $2.1 \pm 1.4$ , and  $2.4 \pm 1.6 \text{ mg l}^{-1}$  (at 6.0, 15.0 and 23.5 m depth) for *in situ* TSM measurements below Research Platform Nordsee in October and November, respectively. Althuis et al. (11) found *in situ* TSM concentrations in the North Sea to range from 0.5 to  $74 \text{ mg l}^{-1}$  with standard deviations of error varying between 0.1 and 6 in several campaigns over a year. Van Raaphorst et al. (19) used *in situ* data having means with standard deviations of  $7.1 \pm 16.4$ ,  $7.4 \pm 16.1$ , and  $14.0 \pm 24.3 \text{ mg l}^{-1}$  for September, and  $22.5 \pm 25.2$ ,  $24.6 \pm 22.9$  and  $22.5 \pm 30.4 \text{ mg l}^{-1}$  for January. For this case, the accuracy of individual values from our TSM maps derived from remote sensing data compare favourably to those of the *in situ* measurements.

### Large-scale processes

The results also show that information about large-scale processes, such as supply (Figures 4-6), transport (Figures 7,8), and deposition (Figures 9,10) can be derived by interpretation of the TSM maps. The interpretation of the TSM maps was compared to similar interpretations based on TSM from *in situ* measurements (1,2,17,18,20). To a large extent we come to comparable conclusions, but information from remote sensing data has also given some new insights. In our studies (4,8) we found, for example, that the form and impact of the East Anglian plume (Figure 7) differ from

estimations (interpolations) from *in situ* measurements (2,24). This was particularly clear for the area north of the westernmost Dutch Wadden Islands. Over here, the tail of the East Anglian plume is located closer to the shore (Figure 7) than found from interpolation of the *in situ* measurements. This could be due to problems with the interpolation of the *in situ* measurements, which might be solved with a geo-statistical technique that uses remote sensing data to improve the interpolation of *in situ* measurements (23). In our study, remote sensing imagery has also shown that "deposition areas" (17,18) can also be suppliers of sediment for further transport depending on the weather conditions and the season (compare Figures 9,5). Van Raaphorst et al. (23) also observed this for the East Anglian plume North of the Dutch Wadden islands. Therefore, SeaWiFS images have proven to be also a useful source of information on sediment dynamics when TSM concentration patterns are related to large-scale processes.

### Budgets

One step further is to derive budgets, and fluxes of sediment transport (in tons yr<sup>-1</sup>) for the North Sea. When using *in situ* data (17-20), however, this step is associated with large uncertainties and a considerable error margin. Eisma (17) mentions the uncertainties in amounts of sediment supplied by seafloor erosion and in sedimentation rates. Dyer & Moffat (20) mention an error of 50 % in their assessment of suspended matter transport in the East Anglian plume. In this light, the potential of the TSM information derived from remote sensing data with its strength in both 2D spatial and temporal coverage (in our study: an average sampling of 107 data sets per pixel over a total of 491 TSM data sets for 2001) is worth further exploration also for the derivation of budgets and assessment of sediment fluxes.

Moreover, remote sensing provides already information about volumes, as concentrations are derived from the near-surface "layer" (as explained in the Introduction). Concentrations in the near-surface layer are, in principle, not representative for the total water column, and especially not in case of stratification. For the southern North Sea, however, an assumption of vertical homogeneity in the water column can be made for the southern waters that occur in a region of thorough mixing. In those cases, concentrations in the near-surface layer could also be used as a first estimate for the derivation of budgets and assessment of sediment fluxes over the total water column. Based on the present study, further use of SeaWiFS data in combination with models (data assimilation) for such investigations seems promising.

### ACKNOWLEDGEMENTS

This paper results from work done for the Noordzee Atlas 2001 project, which was funded by the Survey Department (Meetkundige Dienst) of the Ministry of Transport, Public Works and Water Management of The Netherlands. The authors would like to thank the SeaWiFS Project (Code 970.2) and the Distributed Active Archive Center (Code 902) at the Goddard Space Flight Center, Greenbelt, MD 20771, for the production and distribution of these data, respectively. These activities are sponsored by NASA's Mission to Planet Earth Program. NASA also provided the SeaDAS processing software, and MUMM kindly provided the MUMM atmospheric correction extension. Special thanks to Robert Vos, Jo Suijlen, Hans Roberti, Hans Hakvoort, and Martien Baars for helpful discussions. Finally, we thank Rainer Reuter and an anonymous reviewer for reviewing the manuscript.

### REFERENCES

- 1 Eisma D, 1993. Suspended Matter in the Aquatic Environment. (Springer-Verlag, Berlin)
- 2 Suijlen J M & R N M Duin, 2001. Variability of near-surface total suspended-matter concentrations in the Dutch coastal zone of the North Sea: Climatological study on the suspended matter concentrations in the North Sea. Report RIKZ/OS/2001.150X (RIKZ, The Hague)
- 3 Holligan P M, T Aarup & SB Groom, 1989. The North Sea: satellite colour atlas. Continental Shelf Research, 9: 667-765

- 4 Pasterkamp R, M Eleveld, H van der Woerd, H. & M van Drunen, 2003. Noordzee-atlas voor zwevend stof op basis van satellietbeelden in 2001. Report AGI-GAR-2003-38 (Adviesdienst Geo-informatie en ICT, Delft)
- 5 ICONA (Interdepartmental Co-ordinating Committee for North Sea Affairs), 1992. North Sea atlas for Netherlands policy and management. (Stadsuitgeverij Amsterdam, Amsterdam)
- 6 Ruddick K G, F Ovidio & M Rijkeboer, 2000. Atmospheric Correction of SeaWiFS Imagery for Turbid Coastal and Inland Waters. Applied Optics, 39(6): 897-912
- 7 Van der Woerd H J, J H M Hakvoort, H J Hoogenboom, A Q A Omzigt, R Pasterkamp, S W M Peters, K Ruddick, C de Valk & R J Vos, 2000. Towards an operational monitoring system for turbid waters: POWERS Final Report. Rapportnummer O-00/16 (VU-IVM, Amsterdam)
- 8 Van der Woerd H & R Pasterkamp. Mapping of the North Sea turbid coastal waters using SeaWiFS data. Canadian Journal of Remote Sensing, 30(1): 44-53
- 9 Gordon H R, O B Brown & M M Jacobs, 1975. Computed relationships between the inherent and apparent optical properties of a flat homogeneous ocean. Applied Optics, 14 (2): 417-427
- 10 Ruddick K G, F Ovidio, A Vasilkov, C Lancelot, V Rousseau & M. Rijkeboer, 1999. Optical remote sensing in support of eutrophication monitoring in Belgian waters. In: Operational remote sensing for sustainable development, edited by G J A Nieuwenhuis, R A Vaughan and M Molenaar (Balkema, Rotterdam) 445-452
- 11 Althuis IJ A, J Vogelzang, M R Wernand, S J Shimwell, W W C Gieskes, R E Warnock, J Kromkamp, R Wouts & W Zevenboom, 1996. On the colour of Case 2 waters. Particulate matter North Sea: Part 1 - Results and conclusions. Report number BCRS 95-21A (BCRS, Delft)
- 12 Postma H, 1967. Sediment transport and sedimentation in the estuarine environment. In: Estuaries, edited by G H Lauff (American Association for the Advancement of Science, Publication 83, Washington, DC) 158-179
- 13 RIKZ & RIZA (National Institute for Coastal and Marine Management & Institute for Inland Water Management and Waste Water Treatment), 2003. Waterbase. <http://www.waterbase.nl>
- 14 KNMI (Royal Netherlands Meteorological Institute), 2003. Potential wind means for K13: Corrected to the wind speed at 10 m height over open water with roughness length 0.002 m. (KNMI HYDRA Project: Wind climate assessment of the Netherlands) <http://www.knmi.nl/samenw/hydra>
- 15 Peeters J C H, H Haas, L Peperzak, & L P M J Wetsteyn, 1991. Limiting factors for phytoplankton in the North Sea. Water Science & Technology, 24:262-267
- 16 Pasterkamp R, S W M Peters & H van der Woerd, 2001. Classificatie van watertypes in de Noordzee: Onderzoek naar de detectie van verhoogde algenconcentraties in SeaWiFS opnamen van de Noordzee. Report number O-01/13 (VU-IVM, Amsterdam)
- 17 KNMI (Royal Netherlands Meteorological Institute), 2001. Achtergrond: Zeer zware windstoten op 28 december 2001 en de gevolgen van de storm voor Schiphol. <http://www.knmi.nl/voori/nader/zeerzwarewindstoten28dec2001.htm>
- 18 König P, A Frohse & H Klein, 1994. Measurements of suspended matter dynamics in the German Bight. In: Circulation and contaminant fluxes in the North Sea, edited by J Sündermann (Springer-Verlag, Berlin) 250-270
- 19 Van Raaphorst W, C J M Philippart, J P C Smit, F J Dijkstra, & J F P Malschaert, 1998. Distribution of suspended particulate matter in the North Sea as inferred from NOAA/AVHRR reflectance images and in situ observations. Journal of Sea Research, 39: 197-215
- 20 Suijlen J M & R N M Duin, 2002. Atlas of near-surface total suspended matter concentrations in the Dutch coastal zone of the North Sea. Report RIKZ/2002.059 (RIKZ, The Hague). <http://www.rikz.nl/thema/ikc/rapport2002/rikz2002059.html>